

Synthesis and Spectroscopy of Novel Branched Fluorescent Dyes Containing Benzophenone Parts and the Possibility as Fluorescence Probes

Fang Gao · Lanying Niu · Nvdan Hu · Jianchao Wang ·
Hongru Li · Shengtao Zhang

Received: 15 March 2010 / Accepted: 22 June 2010 / Published online: 29 June 2010
© Springer Science+Business Media, LLC 2010

Abstract This paper describes a new fluorescent family of branched dyes containing benzophenone unit including 4-N, N-diphenylamino-4'-phenacyl-stilbene (**C1**), 4,4'-di(4-benzoylphenylethylene)yl-triphenylamine (**C2**) and 4,4',4''-tri(4-benzoylphenylethylene)yl-triphenylamine (**C3**). Benzophenone part is coupled with core through C–C double bond. The chemical structures of the derivatives are characterized with ^1H and ^{13}C nuclear magnetic resonance and elemental analysis. Strong π – π stacking interactions are discovered with the analysis of the X-ray crystallographic data of **C1**. The absorption maxima and emission maxima of the derivatives exhibit gradual bathochromic shift from **C1** to **C3**. The optical density of **C1**, **C2** and **C3** are shown to be related to the number of branches. The changes of dipole moments between the excited and ground states for **C1**, **C2** and **C3** were estimated to be 4.356, 8.091 and 8.479 Derby, respectively by Lippert equation, confirming that the internal charge transfer (ICT) dominates the process of excited singlet state. The possibility as fluorescence probes of the derivatives on the estimation of what region of micelles interacting with samples was evaluated.

Keywords Synthesis · Spectroscopy · Benzophenone · Branched compound · Fluorescence probe · Micelle

F. Gao (✉) · L. Niu · N. Hu · J. Wang · H. Li (✉) · S. Zhang
College of Chemistry and Chemical Engineering,
Chongqing University,
Chongqing 400044, China
e-mail: fanggao1971@gmail.com
e-mail: hrli@cqu.edu.cn

N. Hu
Department of Environmental and Chemical Engineering,
Liupanshui Normal College,
Guizhuo 553004, China

Introduction

It is of significance to design and synthesize highly fluorescent organic dyes due to their fascinating functions as fluorescence sensors [1–5], biomarkers [6–8], organic electroluminescence devices (OLED) [9–14] and non-linear optical materials [15–17] and so on. Fluorescent dyes, whose emission spectra and fluorescence quantum yields are often markedly sensitive to solvent polarity [18–21], are important for the investigation of chemical, biochemical, and biological phenomena as probes. Although different applications requirements may vary, for most applications an ideal dye should have spectral characteristics such as high fluorescence quantum yield and large molar extinction coefficient, thus it is possible to use of lower dye concentrations in application.

Many efforts have been devoted to improve optical properties of several fluorescent families of dyes including perylene [22–25], rhodamine [26–28] and coumarin [29–31], which are currently applied in chemistry, biomedical and material fields intensively. While to meet the vast requirements as fluorescence devices in various fields, the development of new class of highly fluorescent dyes is needed urgently. A common strategy of molecular design of the photofunctional fluorescent compounds is to couple the functional molecule with a known chromophore group. However, this generally causes fluorescence attenuation of chromophore part due to interaction of chromophore part and functional molecule [32, 33]. Recently, we were interested in developing chromophore part-linked benzophenone compounds with bridged single bond because the fluorescent quantum yields could be enhanced abnormally via the introduction of benzophenone part caused by the enhanced molecular rigidity although benzophenone is a typical triplet compound [34]. In our continuous efforts to develop such derivatives, we propose that the emission of

such branched diphenylethylene derivatives containing benzophenone moiety via C–C double bond could be improved by the enhancement of conjugation nature. Of our particular interests are if the optical properties of such derivatives are related to the number of branches enhanced, and if it is possible to act as fluorescence probes. Many dyes were chosen as fluorescence probes on the evaluation of the viscosity and polarity of micelles, while the probed results sometimes exhibit large difference from each other. The main reason could be due to different encapsulated regions of the probes in micelles, which depends on: (1) neutral *vs* zwitterionic nature, (2) hydrophobic *vs* hydrophilic nature, and (3) large *vs* small size of micelles and probes.

Herein, we report a series of high fluorescent dyes containing benzophenone part which have different zwitterionic and hydrophobic nature, and different molecular sizes. The dyes, 4-N,N-diphenylamino-4'-phenacyl-stilbene, 4,4'-di(4-benzoylphenylethylene)yl-triphenylamine and 4,4',4''-tri(4-benzoylphenylethylene)yl-triphenylamine are shown in Fig. 1. The presence of donor-acceptor moiety in new derivatives caused by the electron-withdrawing effect of carbonyl group in benzophenone unit could induce a large internal charge transfer, so the optical properties of the derivatives could be sensitive to environment, which could make it possible for the derivatives to use as fluorescence probes. Singlet crystal of **C1** was obtained and its X-ray crystallography was determined and discussed. The spectroscopic properties of the derivatives were investigated in various solvents, and the possibility of the derivatives as fluorescence probes was preliminary evaluated.

Experimental

Reagents

The organic solvents were purchased from Chongqing Oriental Chemical Corporation and dried using standard

laboratory techniques according to the published methods [35]. Other reagents were obtained from Aldrich unless otherwise specified. **C1**, **C2** and **C3** (Fig. 1) were synthesized in our laboratory.

Instruments

The UV/visible absorption spectra were recorded with a Cintra spectrophotometer. The emission spectra were checked by Shimadzu RF-531PC spectrofluorophotometer. Rodamin 6G in ethanol ($\Phi=0.94$, 1×10^{-6} – 1×10^{-5} mol/l [36]) acted as reference to determine the fluorescence quantum yields of the derivatives. The melting point was determined using a Sichuan University 2X-1 melting point apparatus. Nuclear magnetic resonance (NMR) was done at room temperature with a Bruker 500 MHz apparatus with tetramethylsilane (TMS) as internal standard and CDCl_3 as solvent. Element analysis was determined with CE440 elemental analysis meter of Exeter Analytical Inc. The fluorescence quantum yields of the compounds in solvents with different polarities were measured based on the following equation [37, 38]:

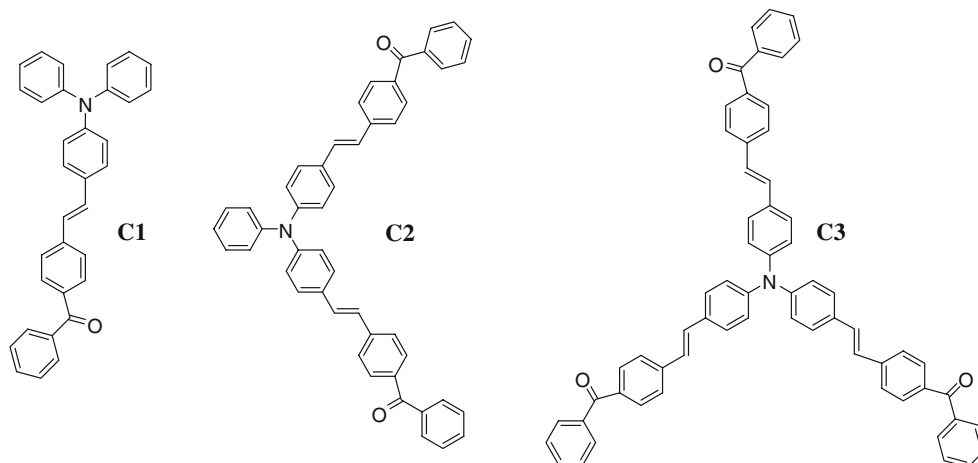
$$\Phi_f = \Phi_f^0 \frac{n_0^2 A^0 \int I_f(\lambda_f) d\lambda_f}{n^2 A \int I_f^0(\lambda_f) d\lambda_f} \quad (1)$$

wherein n_0 and n are the refractive indices of the solvents, A^0 and A are the optical densities at excitation wavelength, Φ_f and Φ_f^0 are the quantum yields, and the integrals denote as the area of the fluorescence bands for the reference and sample, respectively.

Preparation of single crystals and X-ray crystallography

Growing of single crystals of **C1** was done with slow volatilization of benzene solution at 25 °C ($c=1 \times 10^{-2}$ mol/L). The crystal structure of the title compound was determined by X-ray single crystal diffraction. XRD

Fig. 1 Chemical structures of compounds **1** to **3**



data were collected on a Bruker-AXS CCD area detector equipped with diffractometer with Mo K α ($\lambda=0.71073$ Å) at 298 K. A single crystal suitable for determination was mounted inside a glass fiber capillary. The structures of the compounds were solved by direct methods and refined by full-matrix least squares on F2. All the hydrogen atoms were added in their calculated positions and all the non-hydrogen atoms were refined with anisotropic temperature factors. SHELXS97 were used to solve the structure and SHELTL were used to refine the structure [39, 40].

Preparation of micellar solutions

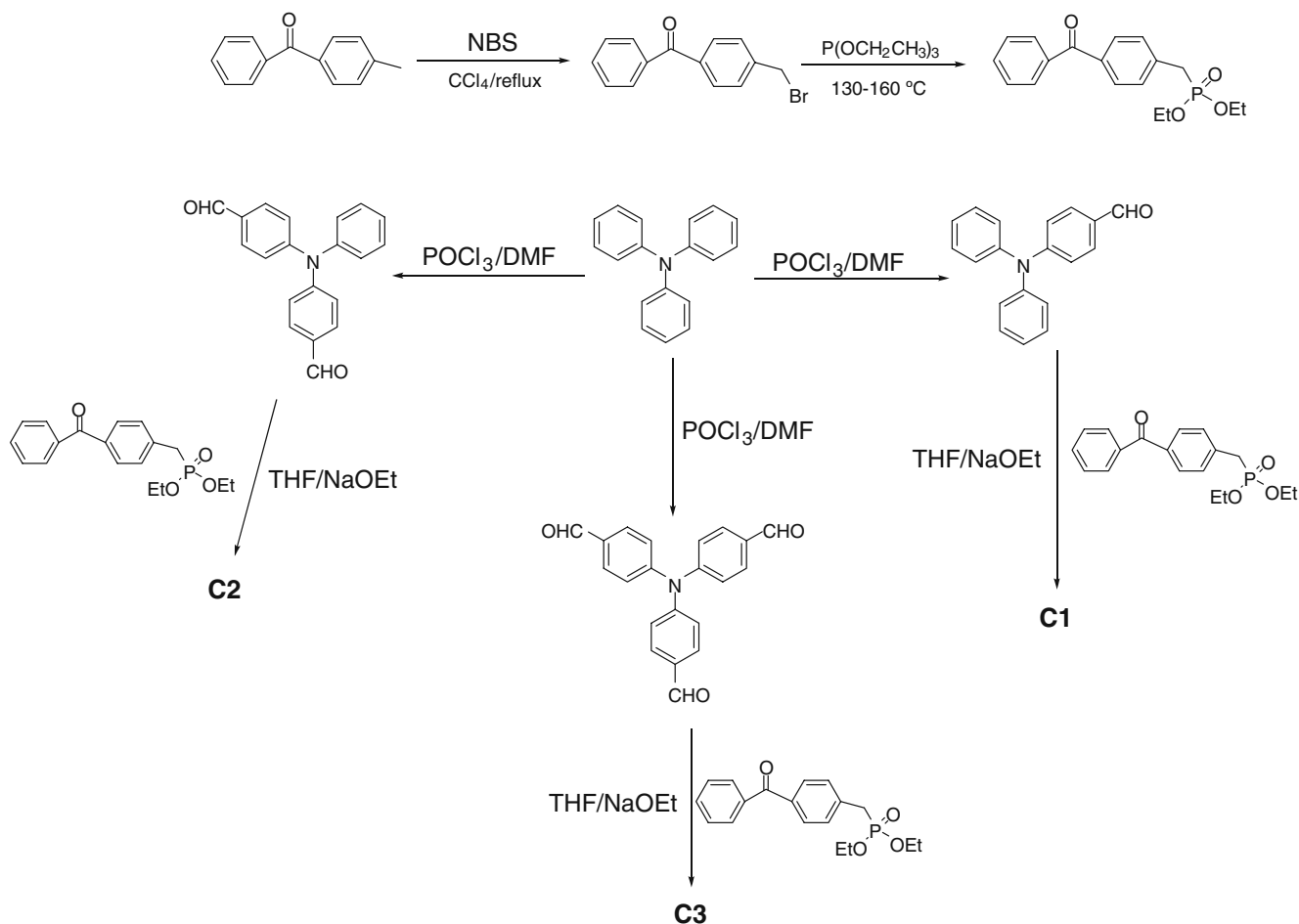
The solutions of the dyes in aqueous detergents were prepared by placing the appropriate amount of chloroform stock solutions (the concentration was 1.0×10^{-5} mol/L for all samples) in a dry volumetric flask, evaporating the solvent with flushing argon, and re-dissolving the residue in the detergent stock solution (the concentration of detergents was 1.0×10^{-2} , 1.0×10^{-3} and 2.0×10^{-3} mol/l for sodium dodecyl sulfate (SDS), cetyltrimethyl ammonium bromide (CTAB) and polyoxyethylene isoctylphenyl ether (TX-100),

respectively) for five hours sonication. Hence, the anionic SDS, neutral TX-100 and cationic CTAB micelles with solubilized dyes (1.0×10^{-5} mol/l) were prepared.

Synthesis of C1 to C3

The synthesis routes of derivatives **1** to **3** were depicted in Scheme 1.

N,N-Diphenyl-benzaldehyde, N-phenyl-N-(*p*-formylphenyl)yl-benzaldehyde and di(*p*-formylphenyl)yl-benzaldehyde were prepared by Veilser reaction using triphenylamine (1.00 g, 4.08 mmol) and restilled POCl₃ (9.5 ml, 101.9 mmol) as starting materials in dry DMF (7.26 ml, 93.8 mmol) [41]. Purification was carried out using benzene/AcOEt mixed solvents ($v:v=30:1$) as eluent. 4-Bromomethylbenzophenone was prepared via bromide of 4-methylbenzophenone with N-bromosuccinimide (NBS) in CCl₄ [42]. It was further purified with recrystallization in benzene/cyclohexane mixed solvents. 4-Bromomethylbenzophenone reacted with excess triethyl phosphite under 130–160°C for 6 h. After excess triethyl phosphite was removed in vacuum, the crude 4-



Scheme 1 Synthesis routes of **C1**, **C2** and **C3**

phosphonate benzophenone was obtained and went directly to the next step with no further purification.

4-*N*, *N*-diphenylamino-4'-phenacyl-stilbene (**C1**)

4-Phosphonate benzophenone (0.939 g, 3 mmol) reacted with *N*, *N*-diphenyl-benzaldehyde (0.903 g, 3 mmol) in dry THF using sodium ethoxide (1.7 g, 20 mmol) as base at room temperature overnight. After the filtration of solid materials and evaporation of THF in vacuum, the reactant mixture was dissolved in chloroform and washed by water. The organic layer was dried with anhydrous magnesium sulphate. After evaporated in vacuum, **C1** was purified with column chromatography using benzene as eluent, which was further purified with recrystallization in methylene chloride. **C1**: color: yellow, yield: 55%, m.p.: 49–51 °C, ¹H-NMR (500 MHz, CDCl₃, δ: ppm, J: Hz): 7.78(d, J=7.0 Hz, 4H, CHCHC), 7.71(d, J=8.5 Hz, 2H, CHCHC), 7.65(t, J=7.5 Hz, 1H, CHCHCH), 7.55(t, J=8.5 Hz, 4H, CCHCH), 7.31(t, J=8.0 Hz, 4H, CHCHCH), 7.22(d, J=16.5 Hz, 2H, CCHCH), 7.08(t, J=7.3 Hz, 6H, CCHCH), 7.00(d, J=8.5 Hz, 2H, CHCHCH). ¹³C-NMR: (123.472, 124.887, 125.741, 126.118, 127.880, 128.484, 129.505, 130.065, 130.943, 131.046, 132.365, 135.983, 138.063, 142.067, 147.504, 148.150, 196.209). Anal. Calcd for C₃₃H₂₅NO, C, 87.77, H, 5.58, N, 3.10, O, 3.54, Found, C, 87.59, H, 5.69, N, 3.21.

4,4'-Di(4-benzoylphenylethylene)yl-triphenylamine (**C2**)

The reaction of *N,N*-diphenyl-benzaldehyde (0.452 g, 1.5 mmol) and 4-phosphonate benzophenone (0.903 g, 3 mmol) was carried out in THF using sodium ethoxide (1.7 g, 10 mmol) as base at room temperature. Purification of **C2** was the same as that of **C1**. **C2**: color: yellow, yield: 53%, m.p. 172–174 °C, ¹H-NMR (CDCl₃): 7.82(t, J=6.8 Hz, 8H, CHCHC), 7.60(t, J=6.8 Hz, 6H, CHCHC), 7.50(t, J=7.5 Hz, 4H, CHCHCH), 7.45(d, J=8.5 Hz, 4H, CCHCH), 7.31(t, J=7.8 Hz, 2H, CHCHCH), 7.21(d, J=16.0 Hz, 2H, CCHCH), 7.16(d, J=8.0 Hz, 2H, CHCHC), 7.10(t, J=9.2 Hz, 6H, CCHCH). ¹³C-NMR: (123.986, 125.332, 126.18, 127.9721, 128.435, 129.650, 130.083, 130.956, 131.440, 132.405, 136.123, 138.50, 141.961, 147.114, 147.628, 196.228). Anal. Calcd for C₄₈H₃₅NO₂, C, 87.64, H, 5.36, N, 2.13, O, 4.86, Found, C, 87.55, H, 5.279, N, 2.03.

4,4',4''-Tri(4-benzoylphenylethylene)yl-triphenylamine (**C3**)

The reaction of di(*p*-formylphenyl)yl-benzaldehyde (0.330 g, 1 mmol) and 4-phosphonate benzophenone (0.903 g, 3 mmol) was performed in dry THF containing sodium ethoxide (1.7 g, 20 mmol) for overnight at room temperature. The purification was carried out as that of **C1** and **C2**. **C3**: color: yellow, yield: 50%, m.p.: 171–172 °C, ¹H-NMR (d⁶-DMSO): 7.75(d, J=10.5 Hz, 18H, CHCHC),

7.68(t, J=7.3 Hz, 3H, CHCHCH), 7.64(d, J=8.0 Hz, 6H, CCHCH), 7.58(t, J=7.0 Hz, 6H, CHCHCH), 7.32(m, J=16.0 Hz, 6H, CCHCH), 7.11(d, J=8.0 Hz, 6H, CCHCH). Anal. Calcd for C₆₃H₄₅NO₃, C, 87.57, H, 5.25, N, 1.62, O, 5.56, Found, C, 87.43, H, 5.19, N, 1.71.

Results and discussion

Synthesis

Formyl groups could be easily introduced to triphenylamine with Vilsmeier reaction. While remarkably low yields of tri(*p*-formylphenyl)yl-benzaldehyde were observed even if much excess of POCl₃/DMF were used. This is mostly caused by the deactivation of the remaining benzene ring by the imine groups on the other two phenyl groups in the third formylation step. The reaction of 4-phosphonate benzophenone and *p*-amino-benzaldehyde easily occurred using sodium ethoxide as base. Stronger base such as sodium hydride led to more byproducts in the final step. Owing to poor solubility in most of solvents caused by excess phenyl rings of **C2** and **C3**, the purification and characterization had to be carried out carefully.

X-ray crystallographic analysis

The asymmetric unit contains one crystallographically unique organic product, one propa-1, 2-diene molecule and one solvent molecule, benzene (Fig. 2). Crystallographic disorder of single crystal of **C1** induce that two carbon have two positions ((C14), and C(14)'), (C(15), and C(15)'), which have 50% rate of the occupancy respectively. The organic product consists of five phenyl rings. As shown in Figs. 2 and 3, rings 1–5 were composed of C atoms from C2 to C7, C8 to C13, C16 to C21, C22 to C27 and C28 to C33, respectively. Rings 1 and 3 are almost coplanar (Dihedral angle: 16.3°). The dihedral angles between planes 1 and 2, 2 and 4, 2 and 5 were 58°, 61.8° and 69.1°, respectively. X1 and X2 are the centers of rings 2 and 4. The X1⋯H27A and X2⋯H33B distance are 3.194 Å and 3.007 Å, respectively (atom with additional labels A, B refers to the symmetry operations. A: x-1, 1.5-y, 0.5+z; B: x, 1.5-y, z-0.5), indicating strong edge-to-face π-π stacking interactions existed (Fig. 3).

UV/visible absorption spectroscopy

Due to electron-withdrawing effect of carbonyl group in benzophenone unit and electron-donating effect of N core, the derivatives exhibit typical D-π-A character. As shown in Fig. 4, a gradual red-shift of the maximal absorption

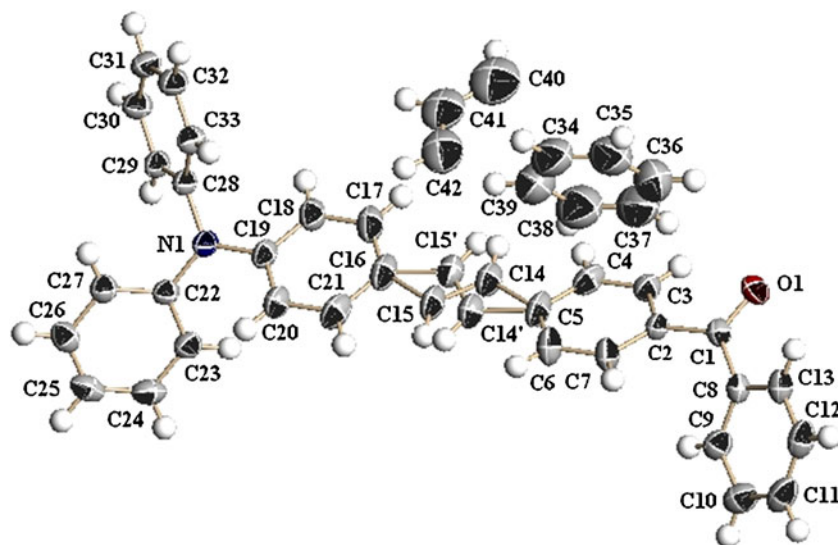
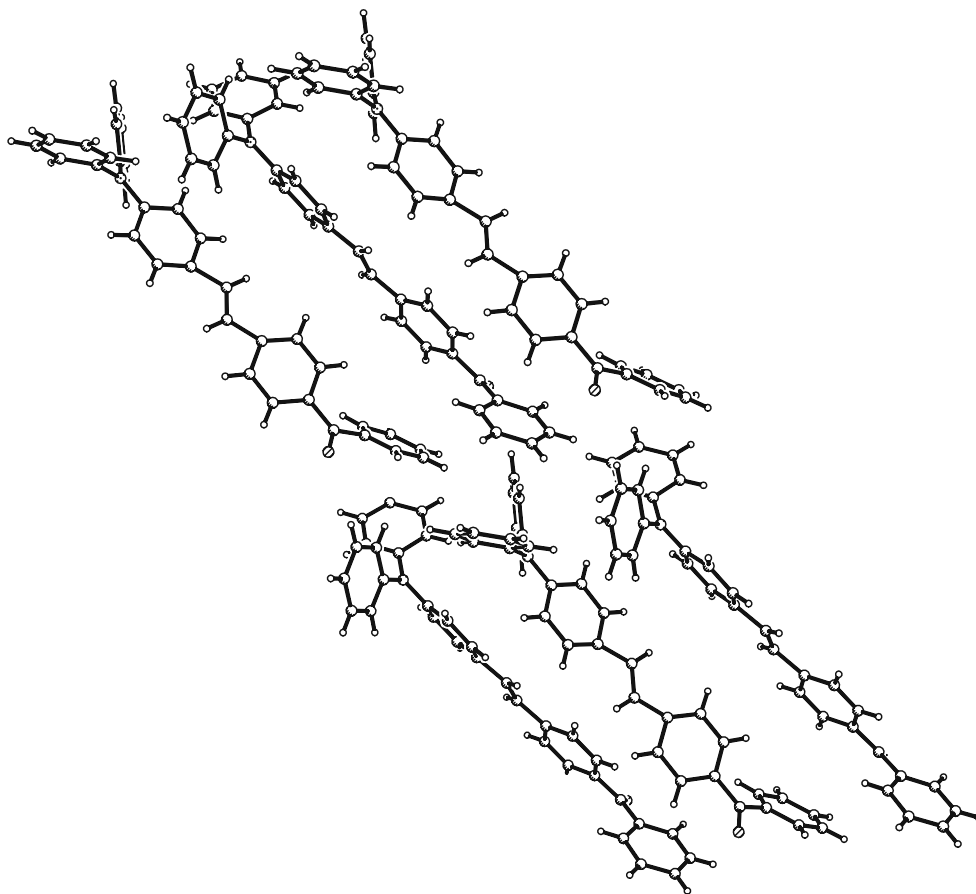


Fig. 2 ORTEP drawing of C1 with thermal ellipsoids at 50% probability

wavelength indicates that there exists internal charge character of (π , π^*). Three absorption bands are observed for the derivatives. The first absorption band from 225–275 nm could be attributed to benzophenone part, and its optical density increases with the increasing number of the branches. It is amazing to observe that the optical density of the second

absorption band 275–350 nm also increases with the number of the branches although the derivatives have only one triphenylamine part. We further determined the UV/visible absorption of different molar ratio triphenylamine/4-methylbenzophenone (1:1, 1:2, 1:3), and no large change on the second absorption of 275–350 nm was observed with the

Fig. 3 π - π Stacking interactions in C1



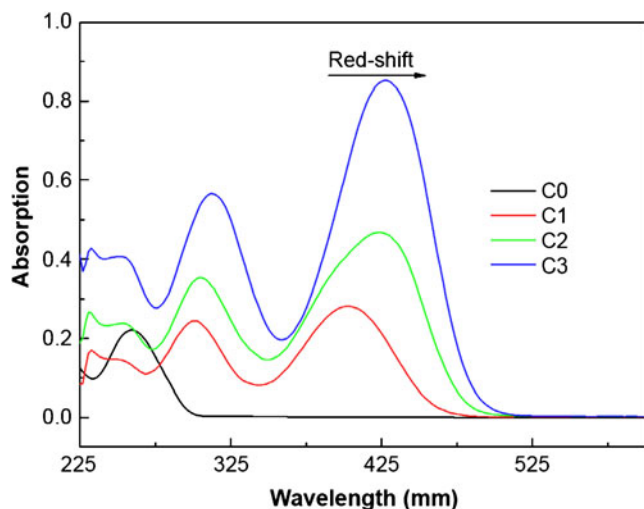


Fig. 4 Absorption spectroscopy of the derivatives and 4-methylbenzophenone in methylene chloride $c: 1 \times 10^{-5}$ mol/L (**C0**: 4-methylbenzophenone, in black line, **C1**: in red line, **C2**: in green line, **C3**: in blue line)

increasing molar of 4-methylbenzophenone. Hence, the absorption band of 275–350 nm could not be simply assigned to triphenylamine core. The second band may be from the overlap of local electron transition of triphenylamine core and overall molecular (π, π) transition, thus the optical density of this absorption band is enhanced with the increasing of the number of the arms. The optical density of third absorption band from (350–525 nm), namely, the maximal absorption band, shows a linear increasing with the number of arms of the derivatives. Furthermore, Table 1 shows that the maximal emission exhibits somewhat bathochromic shift with the increasing of solvent polarity. The results suggest the molecular (π, π) transition has internal charge transfer character [43]. The data demonstrate that that the ratio of the molar extinction coefficients of derivatives is close to the ratio of the number of arms, namely 1:2:3. It could be easily understood from their chemical features. **C1**, **C2** and **C3** are characterized by D- π -A, D-(π -A)₂, D-(π -A)₃ respectively. This results in the cooperative effect on the molar extinction coefficients of derivatives 2 and 3.

Fluorescence spectroscopy and the fluorescence quantum yields

The maximal emission maxima of **C1**, **C2** and **C3** exhibit gradual red-shift in various solvents from the derivatives 1 to 3, as shown in Fig. 5. As compared with the maximal emission wavelength of the derivatives in low polar solvents, it exhibits remarkable red-shift in polar solvents, as shown Table 2. The results imply that large internal charge transfer occurs in the excited singlet state of the derivatives, which means a large dipole moment exists in the excited state. This could be mainly ascribed to donor-acceptor moiety effect as coupling with benzophenone part through double bond. The change of the dipole moments between the excited state and the ground state can be estimated based on Lippert equation [44, 45]:

$$hc(\nu_{abs} - \nu_{em}) = \frac{2(\mu_e - \mu_g)^2}{4\pi\epsilon_0 a^3} \Delta f + const \quad (2)$$

$$\Delta f = \left(\frac{\epsilon - 1}{2\epsilon + 1} - \frac{n^2 - 1}{2n^2 + 1} \right) \quad (3)$$

Wherein h is Planck's constant, c is the speed of light, and Δf is called as the orientation polarizability. ν_{abs} , ν_{em} are the wavenumbers of the absorption and emission, n is the refractive index, and ϵ is the relative low-frequency dielectric constant of the solvents. In Lippert equation, chromophore acts as a dipole, which locates in a cavity with a radius of a in a continuous solvent-dipole environment, and this equation presents a solvent effect of the index of refraction and relative dielectric constant. Consequently, the linear correlation between Stokes shifts and Δf do not reflect some special interaction between the fluorophore and solvent molecules such as hydrogen bonding.

Lippert plots of the derivatives are presented in Fig. 6, in which larger spectral shifts are observed. The linearity of the plot is strong evidence for the dominant importance of solvent effects in the spectral shifts, and three equations are

Table 1 Absorption spectral data of the derivatives in various solvents

Solvents	C1		C2		C3	
	λ_{max} (abs)	$10^{-5} \epsilon$	λ_{max} (abs)	$10^{-5} \epsilon$	λ_{max} (abs)	$10^{-5} \epsilon$
Benzene	395	0.215	417	0.502	420	0.783
Ethyl acetate	391	0.232	414	0.460	415	0.914
Tetrahydrofuran	396	0.255	418	0.470	422	0.843
Methylene chloride	420	0.268	423	0.507	425	0.815
Acetonitrile	393	0.282	416	0.554	424	–

ϵ mol⁻¹·l·cm⁻¹

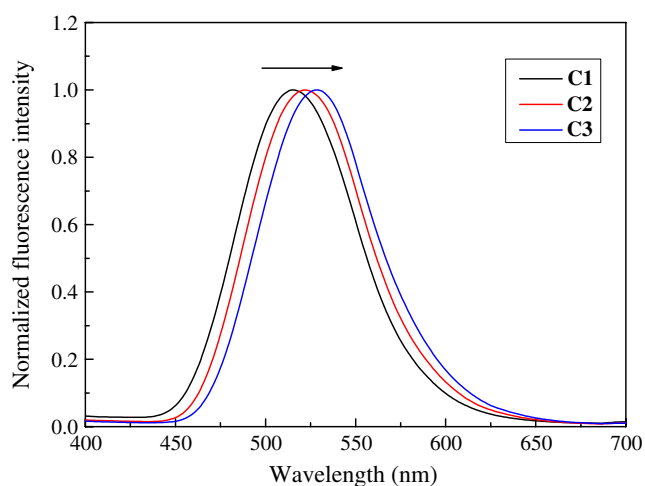


Fig. 5 Emission spectroscopy of the derivatives in THF

obtained as: **C1**: $Y=9635.5X+4142.6$, **C2**: $Y=11573X+2760.9$, **C3**: $Y=11377X+2911.3$. The estimated changes of the dipole moments between the ground and excited singlet states confirm a great internal charge transfer and a large conformational change in the excited state (Table 3). The order of the change of dipole moments decreases gradually from the derivatives 3 to 1. This could explain the gradual red-shift of the maximal absorption and fluorescence wavelength from the derivatives 1 to 3.

As our expectation, the derivatives exhibit strong fluorescence in low-polar solvents. The relative fluorescence quantum yields of the derivatives nearly reach 1.00 in benzene, while the fluorescence quantum yields are reduced in methylene chloride and acetonitrile (Table 2). Such variation of the fluorescence quantum yields suggests that two mechanisms could dominate the decay of the excited singlet state of the derivatives [46, 47]. One is a so-called “negative solvatokinetic effect”, which relates to the decreasing in the fluorescence quantum yields with the suitable enhancement of the internal charge transfer. In other words, in non-polar solvents, the radiative transition decay of the excited state plays significant role. The other

Table 2 The fluorescence spectral data of compounds 1, 2 and 3 in various solvents

Solvents	C1		C2		C3	
	λ_{\max} (em)	Φ	λ_{\max} (em)	Φ	λ_{\max} (em)	Φ
Benzene	480	0.990	481	0.995	483	0.996
Ethyl acetate	514	0.982	520	0.848	524	0.717
Tetrahydrofuran	518	0.927	522	0.877	528	0.695
Methylene chloride	542	0.541	546	0.348	549	0.253
Acetonitrile	559	0.153	562	0.0065	587	–

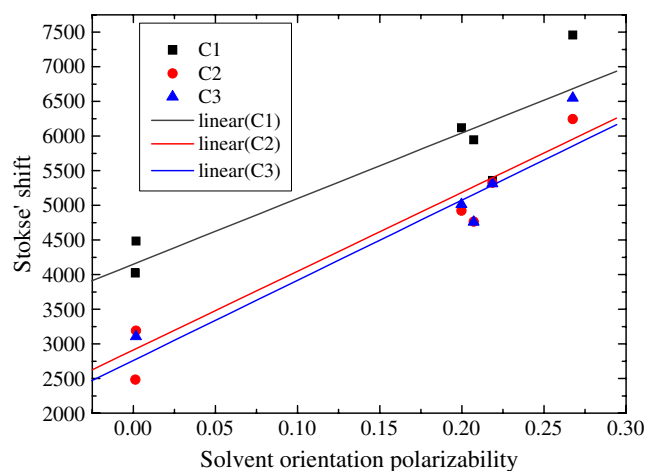


Fig. 6 Relationship between Stokes' shifts of the derivatives and the orientation polarizability (Δf) of solvents respectively

mechanism is a so-called “positive solvatokinetic effect”, according to which, fluorescence quantum yields are much reduced by the strong intra-molecular charge transfer for the larger polarity of solvents. As the attaching benzophenone unit to core through C–C double bond, **C1**, **C2** and **C3** show D- π -A, D-(π -A)₂, D-(π -A)₃ character respectively and thus **C2** and **C3** show larger internal charge transfer nature at the excited states due to branch cooperative effect. Generally, internal charge transfer of organic compounds is strongly dependent on the solvent polarity [48], thus the emission of **C2** and **C3** should be more sensitive to solvent polarity. As shown in Fig. 7, the emission of **C3** varies larger change with the increasing of methylene chloride volume ratio in benzene/methylene chloride binary solvents than that of **C1**.

We have to point out that the fluorescence quantum yields of the derivatives 1 to 3 are much larger than that of simple stilbene, and even greater than stilbenoid dendrimers carrying with dibutylamino groups [49]. It is well demonstrated that for a simple stilbene, *cis-trans* isomerization is the main approach of de-activation of the excited singlet states [50]. In the present study, “internal charge transfer” might dominate the decay of the excited singlet states rather than “*cis-trans*” twist due to “D- π -A” nature of the derivatives as the withdrawing effect of carbonyl group in benzophenone unit. Furthermore, the stiffness, rigidity and conjugation of the derivatives are enhanced by the benzophenone part. As a consequence, the derivatives exhibit strong fluorescence emission in non-polar solvents.

Table 3 Estimated Changes of dipole moments between the ground and the excited states of the derivatives from Lippert equation

The change of dipole moments	C1	C2	C3
$\Delta\mu$ (Derby)	4.356	8.091	8.479

$$1 D = 3.336 \times 10^{-30} \text{ c.m}$$

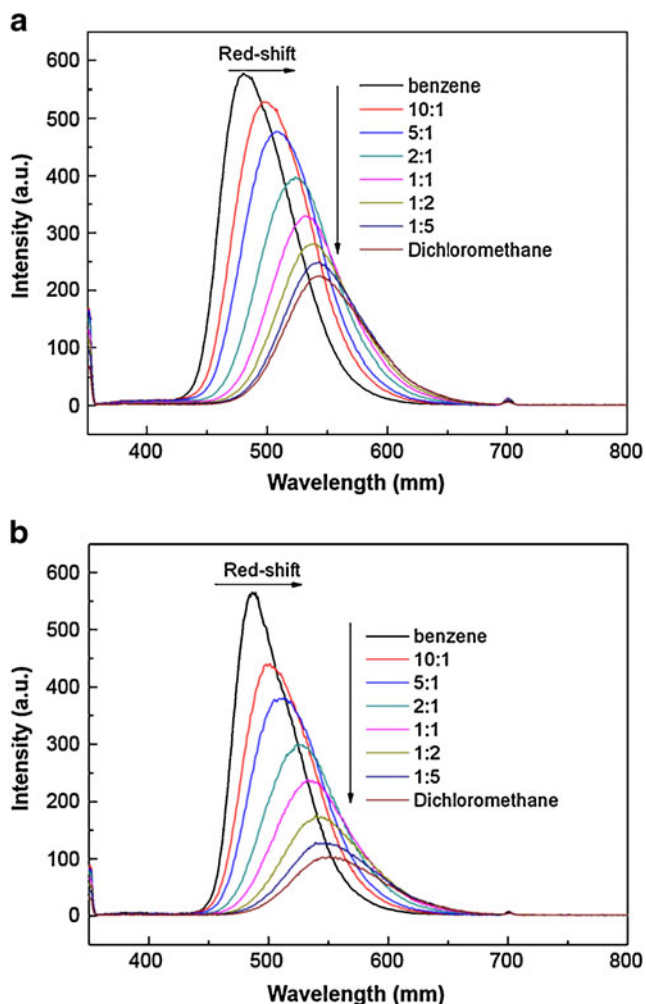


Fig. 7 Typical comparison of variation of emission spectroscopy of **C1** and **C3** with the increasing volume of methylene chloride into benzene/methylene chloride binary solvents

Possibility as fluorescence probes

The UV/visible absorption and fluorescence spectroscopy of the derivatives in anionic, neutral and cationic micelles were determined. The fluorescence quantum yields were also measured. The spectroscopic data in micelles are presented in Table 4. The derivatives display remarkably different maximal absorption and fluorescence wavelength in the same micelle. For instance, in TX-100 micelle, the

Table 5 Some characteristics of **C1**, **C2** and **C3**, and some conventional probes and newly developed fluorescence probes

Fluorescence probes	Size	Charge state	Water solubility
C1	Medium	Zwitterionic	Hydrophobic
C2	Large	Zwitterionic	Hydrophobic
C3	Large	Zwitterionic	Hydrophobic
Pyrene-dendrimer [55]	Huge	Neutral	Hydrophobic
Water-soluble Nile blue [56]	Medium	Ionic	Hydrophilic
DBANS [57]	Medium	Zwitterionic	Hydrophobic
APM [58]	Medium	Zwitterionic	Hydrophobic
Diarylene derivatives [59]	Large	Ionic	Amphiphilic
Nile-red [60, 61]	Medium	Zwitterionic	Hydrophobic
Pyrene [61]	Small	Neutral	Hydrophobic
Nile blue [56]	Medium	Zwitterionic	Hydrophobic
Coumarin 500 [62]	Small	Neutral	Hydrophobic
ANS [62, 63]	Medium	Ionic	Hydrophilic
Dansylamide [61, 64]	Small	Zwitterionic	Amphiphilic

DBANS (4,4'-(*N,N*-dibutylamino)-(*E*)-nitrostilbene, *APM* aminophenoxazine maleimide, *ANS* 8-anilino-1-naphthalene sulfonic acid

maximal UV/visible absorption wavelength of **C3** displays approximate 19 nm red-shift with respect to that of **C2**, and approximate 46 nm red-shift with respect to that of **C1**. A similar phenomenon is observed for the maximal fluorescence emission in various micelles. Furthermore, the maximal absorption and emission wavelength of **C1** are red-shifted in ionic micelles with respect to that in neutral micelle. While as contrast, the maximal fluorescence wavelength of **C2** and **C3** does not exhibit large change in various micelles. On the other hand, the fluorescence quantum yields of **C1** in various micelles are larger than those of **C2** and **C3**, and the fluorescence quantum yields of the derivatives in neutral micelle are higher than those in ionic micelles. Furthermore, the fluorescence quantum yields of the derivatives are much reduced in micelles, particularly in ionic micelles, indicating that the encapsulated regions of micelles have a polar nature.

The spectroscopic data in micelles could be used to probe what region of micelles interacting with molecules.

Table 4 Absorption and fluorescence spectral data of the derivatives in various micelles

Micelles	C1			C2			C3		
	$\lambda_{\max(\text{abs})}$	$\lambda_{\max(\text{em})}$	Φ	$\lambda_{\max(\text{abs})}$	$\lambda_{\max(\text{em})}$	Φ	$\lambda_{\max(\text{abs})}$	$\lambda_{\max(\text{em})}$	Φ
TX-100	402	505	0.361	425	524	0.0117	443	538	0.00836
CTAB	407	522	0.153	431	533	0.00611	451	552	0.00362
SDS	408	523	0.125	432	535	0.00537	453	553	0.00287

The results in Table 4 indicate that **C1** lies in hydrophobic regions of micelles, while it is more close to polar head and surface in ionic micelles. This is mostly due to electronic static dipole polarizability between **C1** and polar head of ionic micelles. The spectral properties of **C2** and **C3** suggest that they are much more near around micelle water interface than **C1**, and thus the absorption and fluorescence spectroscopy is much affected by water molecules. This is intrigue because **C2** and **C3** should have stronger hydrophobic characteristics due to more phenyl rings and they should be encapsulated in hydrophobic layer of micelles. While, the results are reasonable if we consider two main factors: (1) **C2** and **C3** have more dipole moments than **C1**, which results in larger electronic static dipole polarizability between **C2** and **C3** and polar head of ionic micelles. (2) The radius of hydrophobic cores of SDS, CTAB and TX-100 are about 16.7 Å, 21.7 Å and 43.5 Å respectively [51–53]. While, the geometry optimization calculation with AM1 method shows **C2** and **C3** have larger molecular size than that of **C1** respectively (the lengths are approximate 17.9 Å, 25.5 Å and 26.5 Å for **C1**, **C2** and **C3** respectively). As a consequence, **C2** and **C3** could be forced to be located at micelle water interface due to large molecular size. It is well accepted that the probed polarities of micelles are mainly determined by the degree of penetration into the micelles. In the present study, although the probed polarities by different derivatives for the same micelle could be different from each other based on the spectroscopic data, the order of polarity (TX-100<CTAB<SDS) is agreement for the different derivatives, which is perfectly consistent with previous report [54]. We would point out the development process of these new fluorescence probes reported herein is not more difficult than that of some newly reported probes [55–59]. We further summarize the characteristics of some conventional fluorescence probes and novel probes. Seen from Table 5, **C1**, **C2** and **C3** are characterized with zwitterionic state and hydrophobic nature, which is quite similar to that of Nile blue [56], DBANS [57], APM [58], Nile red [60, 61] while it is some different from that of pyrene dendrimer [55], aqueous Nile blue [56], diaryethene derivatives [59], pyrene [61], coumarin 500 [62], ANS [62, 63] and dansylamide [60, 64]. Hence, the derivatives reported in the present report could be employed as fluorescence probes in some environments.

Conclusions

To summarize, a class of new fluorescence family carrying benzophenone part through C–C double bond are successfully developed. The X-ray crystallographic confirms the presence of strong face-to-edge π - π stacking effect for **C1**.

Owing to electron-withdrawing effect of carbonyl group in benzophenone moiety, (π , π) transition of the derivatives exhibits internal charge transfer nature, which could be tuned by the variation of the number of arms, and thus the spectral properties could be regulated. Our results demonstrate that the derivatives could be employed as efficient fluorescence probes to determine what region of micelles interacting with molecules.

Supporting materials

CCDC 713270 contains the supplementary crystallographic data for this paper. These data can be obtained free of charge via www.ccdc.cam.ac.uk/conts/retrieving.html or from the Cambridge Crystallographic Data Centre, 12, Union Road, Cambridge CB2 1EZ, UK; fax: 44 1223 336033).

Acknowledgements The authors appreciate financial support from National Natural Science Foundation of China (Nos. 20776165, 20702065, 20872184). We would thank “the Foundation of Chongqing Science and Technology Commission” (CSTC2008BA4020, CSTC2009BB4216). We also appreciate warm supports from the Key Laboratory of Functional Crystals and Laser Technology, TIPC, Chinese Academy of Sciences. We also thank “Innovative Talent Training Project, the Third State of “211 Project, S-09103”, Chongqing University.

References

1. Yoon S, Albers AE, Wong AP, Chang CJ (2005) Screening mercury levels in fish with a selective fluorescent chemosensor. *J Am Chem Soc* 127:16030–16031. doi:10.1021/ja0557987
2. Hirano J, Hamase K, Miyata H, Zaitso K (2010) 6, 7-difluoro-1, 4-dihydro-1-methyl-4-oxo-3-quinolinecarboxylic acid, a newly designed fluorescence enhancement-type derivatizing reagent for amino compounds. *J Fluoresc* 20(2):615–624. doi:10.1007/s10895-009-0596-2
3. Pu KY, Pan S, Liu B (2008) Optimization of interactions between a cationic conjugated polymer and chromophore-labeled DNA for optical amplification of fluorescent sensors. *J Phys Chem B* 112(31):9295–9300. doi:10.1021/jp8019717
4. Wang L, Yang X, Zhao M (2009) A 4-methylumbelliferone-based fluorescent probe for the sensitive detection of captopril. *J Fluoresc* 19(4):593–599. doi:10.1007/s10895-008-0449-4
5. Geddes CD (2002) 1 and 2-photon fluorescence anisotropy decay to probe the kinetic and structural evolution of sol-gel glasses: a summary. *J Fluoresc* 12(3–4):343–367. doi:10.1023/A:1021353707955
6. Mukundan H, Xie H, Anderson AS, Grace WK, Shively JE, Swanson BI (2009) Optimizing a waveguide-based sandwich immunoassay for tumor biomarkers: evaluating fluorescent labels and functional surfaces. *Bioconj Chem* 20(2):222–30. doi:10.1021/bc80283e
7. Liu Q, Liu J, Guo JC, Yan XL, Wang DH, Chen L, Yand FY, Chen LG (2009) Preparation of polystyrene fluorescent microspheres based on some fluorescent labels. *J Mater Chem* 19:2018–2025. doi:10.1039/b816963b
8. Anderson J, Nelson J, Reynolds C, Ringelberg D, Tepper G, Pestov D (2005) Steady-state and frequency-domain lifetime

- measurements of an activated molecular imprinted polymer imprinted to dipicolinic acid. *J Fluoresc* 14(3):269–274. doi:10.1023/B:JOFL.0000024558.68095.27
9. Fan Z, Cheng C, Yu S, Ye K, Sheng R, Xia D, Ma C, Du G (2009) Red and near-infrared electroluminescence from organic light-emitting devices based on a soluble substituted metal-free phthalocyanine. *Opt Mater* 31(4):889–894. doi:10.1016/j.optmat.2008.10.023
 10. Vala M, Weiter M, Vynuchal J, Toman P, Lunak S (2008) Comparative studies of diphenyl-diketo-pyrrolopyrrole derivatives for electroluminescence applications. *J Fluorescence* 18(6):1181–1186. doi:10.1007/s10895-008-0370-x
 11. Yao ZB, Zhou Q, Wang X, Wang Y, Zhang B (2007) A DCM-type red-fluorescent dopant for high-performance organic electroluminescent devices. *Adv Funct Mater* 17:93–100. doi:10.1002/adfm.200600055
 12. Feng J, Okamoto T, Kawata S (2005) Highly directional emission via coupled surface-plasmon tunneling from electroluminescence in organic light-emitting devices. *Appl Phys Lett* 87(24):1109. doi:10.1063/1.2142085
 13. Zhou E, Lv Z, Deng Z, Wang H, Xu D, Chen Z, Wei W, Zhang Y (2009) Electroluminescence performance of organic light-emitting devices with KCl inside hole transport layer. *J Lumin* 29(11):1390–1392. doi:10.1016/j.jlumin.2009.07.009
 14. Leung M, Chang C, Wu M, Chuang K, Lee J, Shieh S, Lin S, Chiu C (2006) 6-N, N-diphenylaminobenzofuran-derived pyran containing fluorescent dyes: a new class of high-brightness red-light-emitting dopants for OLED. *Org Lett* 8(12):2623–2626. doi:10.1021/ol060803c
 15. Srinivasan P, Kanagasakaran AT, Vijayan N, Bhagavannarayana G, Gopalakrishnan R, Srinivasan RPP (2007) Studies on the growth, optical, thermal and dielectric aspects of a proton transfer complex—dimethyl amino pyridinium 4-nitrophenolate 4-nitrophenol (DMAPNP) crystals for non-linear optical. *Appl Opt Mater* 30(4):553–564. doi:10.1016/j.optmat.007.01.014
 16. Lee CH, Bihari B, Filler R, Mandal BK (2009) New azobenzene non-linear optical materials for eye and sensor protection. *Opt Mater* 32(1):147–153. doi:10.1016/j.optmat.009.07.001
 17. Martin SA, Dhas B, Natarajan S (2007) Growth and characterization of a new organic NLO material: glycine nitrate. *Opt Commun* 278(2):434–438. doi:10.1016/j.optcom.007.6.052
 18. Olivares SP, Rizzo S, Gutiérrez MI (2008) Solvent Effects on the Spectroscopic Properties of 4-Hexylresorcinol. *Spectrochim Acta Part A* 71(2):336–339. doi:10.1016/j.saa.007.12.037
 19. Toro C, Thibert A, Boni LD, Masunov AE, Hernández FE (2008) Fluorescence emission of disperse red 1 in solution at room temperature. *J Phys Chem B* 112(3):929–937. doi:10.1021/jp076026v
 20. Wu L, Burgess K (2008) Synthesis and spectroscopic properties of rosamines with cyclic amine substituents. *J Org Chem* 73(22):8711–8718. doi:10.1021/jo800902j
 21. Diaz MS, Freile ML, Gutiérrez MI (2009) Solvent effect on the UV/Vis absorption and fluorescence spectroscopic properties of berberine. *Photochem Photobiol Sci* 8:970–974. doi:10.1039/b822363g
 22. Turkmen G, Ela SE, Icli S (2009) Highly soluble perylene dyes: synthesis, photophysical and electrochemical characterizations. *Dyes Pigm* 83(3):297–303. doi:10.1016/j.dyepig.2009.05.014
 23. Zhang X, Rehm S, Sempere MMS, Würthner F (2009) Vesicular perylene dye nanocapsules as supramolecular fluorescent PH sensor systems nature. *Chem Eur J* 1:23–629. doi:10.038/nchem.368
 24. Aoki H, Takahashi T, Tamai Y, Sekine R, Aoki S, Tani K, Ito S (2009) Poly(methacrylate)s labeled by perylene diimide: synthesis and applications in single chain detection studies. *Polym J* 41(9):778–783. doi:10.1295/polymj.PJ2009099
 25. Rajaram S, Armstrong PB, Kim BJ, Frechet JMJ (2009) Effect of addition of a diblock copolymer on blend morphology and performance of poly(3-hexylthiophene): perylene diimide solar cells. *Chem Mater* 21(9):1775–1777. doi:10.1021/cm900911x
 26. Beija M, Afonso CAM, Martinho JMG (2009) Synthesis and applications of rhodamine derivatives as fluorescent probes. *Chem Soc Rev* 38:2410–2433. doi:10.1039/b901612k
 27. Fu M, Xiao Y, Qian X, Zhao D, Xu Y (2008) ChemInform abstract: a design concept of long-wavelength fluorescent analogues of rhodamine dyes: replacement of oxygen with silicon atom. *Chem Commun* 21:1780. doi:10.1002/chin.200833178
 28. Yang YK, Cho HJ, Lee J, Shin I, Tae J (2009) A rhodamine-hydroxamic acid-based fluorescent probe for hypochlorous acid and its applications to biological imagings. *Org Lett* 11(4):859–861. doi:10.1021/ol802822t
 29. Kandavelu V, Huang HS, Jian JL, Yang TCK, Wang KL, Huang ST (2009) Novel iminocoumarin dyes as photosensitizers for dye-sensitized solar cell. *Sol Energy* 83(4):574–581. doi:10.1016/j.solener.2008.10.002
 30. Lee DN, Kim GJ, Kim HJ (2009) A fluorescent coumarinylalkyne probe for the selective detection of mercury(II) ion in water. *Tetrahedron Lett* 50(33):4766–4768. doi:10.1016/j.tetlet.2009.06.017
 31. Çamur M, Bulut M, Kandaz M, Güney O (2009) Synthesis, characterization and fluorescence behavior of new fluorescent probe phthalocyanines bearing coumarin substituents. *Polyhedron* 28(2):233–238. doi:10.1016/j.poly.2008.10.066
 32. Reitzenstein D, Macromolecules CL (2009) Localized versus backbone fluorescence in N-p-(Diarylboryl)phenyl-substituted 2, 7- and 3, 6-linked polycarbazoles. *Macromolecules* 42(3):773–782. doi:10.1021/ma802232r
 33. Fang L, Li Y, Wang R, Xu C, Li S (2009) Synthesis and photophysical properties of poly(aryleneethynylene)s bearing dialkylsilyl side substituents. *Eur Polym J* 45(4):1092–1097. doi:10.1016/j.eurpolymj.2009.01.010
 34. Gao F, Hu N, Xie T, Cheng Z, Yang L, Liu X, Li Z, Wang X, Li H, Li X (2008) Study of the absorption and emission spectroscopy of “A–B” type photosensitive compounds including two-photon chromophore and benzophenone moiety. *Spectrochimica Acta Part A* 70(5):1006–1012. doi:10.1016/j.saa.2007.07.064
 35. Perrin DD, Armarego WLF, Perrin DR (1966) Purification of laboratory chemicals. Pergamon, London
 36. Fischer M, Georges J (1996) Fluorescence quantum yield of rhodamine 6G in ethanol as a function of concentration using thermal lens spectrometry. *Chem Phys Lett* 260(1–2):115–118. doi:10.1016/0009-2614(96)00838-X
 37. Maus M, Reitigg W, Bonafoux D, Lapouyade R (1999) Photoinduced intramolecular charge transfer in a series of differently twisted donor-acceptor biphenyls as revealed by fluorescence. *J Phys Chem A* 103(18):3388–3401. doi:10.1021/jp9905023
 38. Lukeman M, Veal D, Wan P, Ranjit V, Munasinghe N, Corrie JE (2004) Photogeneration of 1, 5-naphthoquinone methides via excited-state (formal) intramolecular proton transfer (ESIPT) and photodehydration of 1-naphthol derivatives in aqueous solution. *Can J Chem* 82(14):240–253. doi:10.1139/v03-184
 39. Sheldrick GM (1997) SHELXS 97, Program for Crystal Structure Solution University of Göttingen, Göttingen
 40. Sheldrick GM (1997) SHELXL 97, Program for Crystal Structure Refinement University of Göttingen, Göttingen
 41. Mallegol T, Gmouh S, Meziane MAA, Blanchard-Desce M, Mongin O (2005) Practical and efficient synthesis of tris(4-formylphenyl)amine, a key building block in materials chemistry. *Synthesis* 2005(11):1771–1774. doi:10.1055/s-2005-865336
 42. Itoh T, Hall HK (1990) 7-Chloro-7-phenyl-8, 8-dicyanoquinodimethane. A novel initiator for cationic polymerizations. *Macromolecules* 1990(23):4879–4881. doi:10.1021/ma00224a020

43. Wang S, Kim SH (2009) Photophysical and electrochemical properties of D- π -A type solvatochromic isophorone dye for pH molecular switch. *Curr Appl Phys* 9(4):783–787. doi:10.1016/j.cap.2008.07.009
44. Lippert VEZ (1957) Spektroskopische Bistimmung des Dipolmomentes aromatischer Verbindungen im ersten angeregten Singulettzustand. *Z Electrochem* 61:962–975
45. Lakowicz JR (1999) Principles of fluorescence spectroscopy. Kluwer, New York
46. Li ZM, Wu SK (1996) Study on photophysical behaviors of dtyryl pyrazine derivatives. *Acta Phys Chim Sin* 12:418–422
47. Li ZM, Wu SK (1997) The effect of molecular structure on the photophysical behavior of substituted styryl pyrazine derivatives. *J Fluoresc* 7:237–242. doi:10.1007/BF02758224
48. Chatterjee S, Pramanik S, Hossain SU, Blattacharya S, Bhattacharya SC (2007) Synthesis and photoinduced intramolecular charge transfer of N-substituted 1, 8-naphthalimide derivatives in homogeneous solvents and in presence of reduced glutathione. *J Photochem Photobiol A Chem* 187(1):64–71. doi:10.1016/j.jphotochem.2006.09.013
49. Segura JL, Gomez R, Martin N, Guldi DM (2001) Synthesis of photo- and electroactive stilbenoid dendrimers carrying dibutylamino peripheral groups. *Org Lett* 3(17):2645–2648. doi:10.1021/ol1016083l
50. Uda M, Mizutani T, Hayakawa J, Momotake A, Ikegami M, Nagahata R, Arai T (2002) Photoisomerization of stilbene dendrimers: the need for a volume-conserving isomerization mechanism. *Photochem Photobiol* 76:596–605. doi:10.1562/0031-8655(2002)076<0596:POSDTN>2.0.CO;2
51. Ranganathan R, Peric M, Medina R, Garcia U, Bales B (2001) Size, hydration, and shape of SDS/heptane micelles investigated by time-resolved fluorescence quenching and electron spin resonance. *J Phys Chem* 17(22):6765–6770. doi:10.1021/la010231z
52. Tavernier HL, Barzykin AV, Tachiya M, Fayer MD (1998) Solvent reorganization energy and free energy change for donor/acceptor electron transfer at micelle surfaces: theory and experiment. *J Phys Chem* 102(31):6078–6088. doi:10.1021/jp981754r
53. Phillis GDJ, Scott J, Ren SZ (1993) Probe diffusion in the presence of nonionic amphiphiles: Triton X 100. *J Phys Chem* 97(44):11563–11568. doi:10.1021/j100146a034
54. Dennison SM, Guharay J, Sengupta PK (1999) Intramolecular excited-state proton transfer and charge transfer fluorescence of a 3-hydroxyflavone derivative in micellar media. *Spectrochim Acta Part A* 55(4):903–909. doi:10.1016/S1386-1425(98)00314-X
55. Claire MB, Tanja W, Andreas H, Joachim OR, Klaus M (2003) A polyphenylene dendrimer–detergent complex as a highly fluorescent probe for bioassays. *J Am Chem Soc* 125(19):5832–5838. doi:10.1021/ja0285058
56. Jose J, Ueno Y, Burgess K (2009) Water-soluble Nile blue derivatives: syntheses and photophysical properties. *Chem Eur J* 15(2):418–423. doi:10.1002/chem.200801104
57. Berg O, Sengers WGF, Jager WF, Picken SJ, Wübbenhorst M (2004) Dielectric and fluorescent probes to investigate glass transition, melt, and crystallization in polyolefins. *Macromolecules* 37(7):2460–2470. doi:10.1021/ma0305333
58. Cohen BE, Pralle A, Yao XJ, Swaminath G, Gandhi CS, Jan YN, Kobilka BK, Isacoff EY, Jan LY (2004) A fluorescent probe designed for studying protein conformational change. *PNAS* 102:4965–4970. doi:10.1073/pnas.0409469102
59. Zou Y, Yi T, Xiao SZ, Li FY, Li CY, Gao X, Wu JC, Yu MX, Huang CH (2008) Amphiphilic diarylethene as a photoswitchable probe for imaging living cells. *J Am Chem Soc* 130(47):15750–15751. doi:10.1021/ja8043163
60. Krishna MMG (1999) Excited-state kinetics of the hydrophobic probe Nile red in membranes and micelles. *J Phys Chem A* 103(19):3589–3595. doi:10.1021/jp984620m
61. Fletcher KA, Storey IA, Hendricks AE, Pandey S (2001) Behavior of the solvatochromic probes Reichardt's dye, pyrene, dansylamide, Nile red and 1-pyrene-carbaldehyde within the room-temperature ionic liquid bmimPF₆. *Green Chem* 3:210–215. doi:10.1039/b103592b
62. Narayanan SS, Sinha SS, Sarkar R, Pal SK (2008) Validation and divergence of the activation energy barrier crossing transition at the AOT/lecithin reverse micellar interface. *J Phys Chem B* 112:2859–2867. doi:10.1021/jp710127s
63. Griffiths PC, Roe JA, Bales BL, Pitt AR, Howe AM (2000) Fluorescence probe studies of gelatin–sodium dodecyl sulfate interactions. *Langmuir* 16(22):8248–8254. doi:10.1021/la0001833
64. Bae CD, Yoo HJ, Kim SY, Lee KG, Kim JY, Sung MM, Shin HJ (2008) Template-directed synthesis of oxide nanotubes: fabrication, characterization, and applications. *Chem Mater* 20(3):756–767. doi:10.1021/cm702138c